Pten Loss in the Mouse Thyroid Causes Goiter and Follicular Adenomas: Insights into Thyroid Function and Cowden Disease Pathogenesis

Nicole Yeager,[1] Andres Klein-Szanto,[2] Shioko Kimura,[3] and Antonio Di Cristofano[1]

[1]Human Genetics Program and [2]Department of Pathology, Fox Chase Cancer Center, Philadelphia, Pennsylvania and [3]Laboratory of Metabolism, National Cancer Institute, NIH, Bethesda, Maryland

Abstract

Inactivation and silencing of the tumor suppressor *PTEN* are found in many different epithelial tumors, including thyroid neoplasia. Cowden Disease patients, who harbor germ-line *PTEN* mutations, often display thyroid abnormalities, including multinodular goiter and follicular adenomas, and are at increased risk of thyroid cancer. To gain insights into the role *PTEN* plays in thyroid function and disease, we have generated a mouse strain, in which Cre-mediated recombination is used to specifically delete *Pten* in the thyrocytes. We found that *Pten* mutant mice develop diffuse goiter characterized by extremely enlarged follicles, in the presence of normal thyroid-stimulating hormone and T4 hormone levels. Loss of *Pten* resulted in a significant increase in the thyrocyte proliferative index, which was more prominent in the female mice, and in increased cell density in the female thyroid glands. Surprisingly, goitrogen treatment did not cause a substantial increase of the mutant thyroid size and increased only to some extent the proliferation index of the female thyrocytes, suggesting that a relevant part of the thyroid-stimulating hormone–induced proliferation signals are funneled through the phosphatidylinositol-3-kinase (PI3K)/Akt cascade. Although complete loss of *Pten* was not sufficient to cause invasive tumors, over two thirds of the mutant females developed follicular adenomas by 10 months of age, showing that loss of *Pten* renders the thyroid highly susceptible to neoplastic transformation through mechanisms that include increased thyrocyte proliferation. Our findings show that constitutive activation of the PI3K/Akt cascade is sufficient to stimulate continuous autonomous growth and provide novel clues to the pathogenesis of Cowden Disease and sporadic nontoxic goiter. [Cancer Res 2007;67(3):959–66]

Introduction

The thyroid gland is characterized by an extremely low proliferation index (1). However, and rather paradoxically, the thyroid is also extremely sensitive to alterations of the equilibrium governing its homeostasis: hyperplastic disorders of this rather quiescent organ affect up to 67% of the U.S. population (2). Increased stimulation of thyroid growth is causally linked to a variety of pathologic conditions, ranging from nodular hyperplasia (goiter) to neoplastic transformation (3).

Requests for reprints: Antonio Di Cristofano, Human Genetics Program, Fox Chase Cancer Center, 333 Cottman Avenue, Philadelphia, PA 19111. Phone: 215-214-1647; Fax: 215-214-1623. E-mail: antonio.dicristofano@fccc.edu.

doi:10.1158/0008-5472.CAN-06-3524

Thyroid growth is primarily induced by the pituitary-derived thyroid-stimulating hormone (TSH), whose levels are regulated by the thyroid hormone through a negative feedback mechanism (4). TSH binding to its receptor (TSHR) activates the cyclic AMP (cAMP)/protein kinase A (PKA)–dependent mitogenic cascade, leading to both the induction of cell cycle progression and the expression of differentiation markers (5). Increasing evidence from *in vitro* models indicates that the mitogenic activity of TSH necessitates the cooperation of peptide growth factors, such as insulin-like growth factor-I (IGF-I), epidermal growth factor, insulin, etc. (6). However, the often contradictory results obtained in different cell culture systems have not yet clarified the relative roles and contribution of TSHR- and receptor tyrosine kinase (RTK)–initiated signal transduction pathways to the mitogenic process (7).

Phosphatidylinositol-3-kinase (PI3K) is a central mediator of all RTK-initiated signaling cascades, catalyzing the conversion of phosphatidylinositol (4,5)-biphosphate (PIP-2) into phosphatidylinositol (3,4,5)-triphosphate (PIP-3). The major effector of PI3K is the Akt kinase, which is activated upon PIP-3–mediated membrane recruitment and, in turn, phosphorylates an ever-growing list of target proteins regulating key processes, such as proliferation, survival, cell size, and mRNA translation (8). This process is counteracted by the PTEN tumor suppressor, which opposes PI3K activity by dephosphorylating PIP-3 to PIP-2 (9). *In vitro* studies have shown that the PI3K/Akt/PTEN signaling pathway is involved in the implementation of the growth factor–dependent proliferative signals in thyroid cells (10, 11). In addition, deregulation of this cascade, through activation of PI3K and Akt and loss of PTEN expression, is frequently found in thyroid cancer (11–17). Finally, heterozygous mutation of *PTEN* causes Cowden disease, a dominant genetic syndrome whose characteristics include thyroid benign disorders, such as multinodular goiter and adenoma, and a 10% lifetime risk for developing thyroid cancer, mostly of the follicular type (18–20).

Despite many correlative data suggest that this signaling cascade plays a central role in the control of normal thyroid function and that its deregulation is linked to thyroid disease, direct *in vivo* evidence supporting this hypothesis is still missing. Moreover, until now, there has been no genetic model that could be exploited to tease out the relative contributions of the two major growth-stimulating signals in the thyroid, TSH and growth factors, and to dissect in a physiologically relevant setting the molecular pathways that are altered in thyroid proliferative lesions.

To address these issues, we have generated a mouse strain, in which the *Pten* gene is selectively deleted in the thyroid follicular cells, thus constitutively activating the PI3K/Akt pathway and reproducing the genetic events taking place in the nodular lesions developing in Cowden disease patients. Our data show that Akt

activation is sufficient, *in vivo*, to induce thyroid hyperplasia and diffuse colloid goiter in young mice by increasing the thyroid mitotic index and to create fertile ground for neoplastic transformation in older mutants.

Materials and Methods

Animals and treatments. Generation of $Pten^{+/-}$, $Pten^{L/L-}$, and thyroid peroxidase (TPO)-Cre mice has been described (21–23). $Pten^{L/L}$ mice in the 129Sv background were initially bred to TPO-Cre mice in the FVB/N background and then backcrossed in the 129Sv background. At different time points, mice were euthanized and weighed. The thyroid was dissected and weighed; one lobe was fixed for pathologic analysis, and the other was frozen in liquid nitrogen. Hypothyroidism was induced at 8 weeks of age by administration of 0.5% sodium perchlorate and 0.05% methimazole (both from Sigma Chemical Co., St. Louis, MO), given in drinking water for 4 weeks. Mice were weighed and killed, and samples were collected as described above.

Real-time PCR. The recombination frequency for the *Pten*-floxed allele was determined as described previously (24). Briefly, two sets of primers were designed to distinguish the floxed allele from the recombined allele (Fig. 1*A*). Reactions with the two primer pairs (D/E and F/G) were done in separate wells of the same 96-well reaction plate using SYBR Green Master Mix (Applied Biosystems, Foster City, CA) and the results were analyzed according to the following formula: % recombined allele = $[1 / (1 + 2^{\Delta CT})] \times 100$, where ΔC_T = recombined C_T − floxed C_T.

Hormone measurements. Blood was collected by cardiac puncture, and serum was stored at −80°C until analysis. TSH and total T4 were measured by radioimmunoassay at the Harbor-University of California at Los Angeles Medical Center (Torrance, CA).

Immunohistochemical analysis. The following rabbit polyclonal antibodies were used: Ki-67 (Vector Laboratories, Burlingame, CA), cyclin D1 (Lab Vision, Fremont, CA), phosphorylated p70S6K, phosphorylated S6, phosphorylated Foxo1, and phosphorylated estrogen receptor α (P-ERα) S167 (Cell Signaling, Danvers, MA); for PTEN and phosphorylated Akt (pAkt) S473, rabbit monoclonal antibodies were used. Tissues were fixed, embedded in paraffin, and sectioned at 6 μm. Sections were subjected to antigen retrieval in 0.1 mol/L sodium citrate and counterstained with hematoxylin.

Morphometric analysis. The H&E-stained sections were photographed at ×100 and ×400 magnification and analyzed using the ImageJ software. The area of at least 100 follicles was determined by measuring the luminal surface. Follicle density was determined by counting different areas to cover 2 to 5 mm^2. Cell density was calculated counting the number of cells in different areas to cover 0.2 to 0.5 mm^2 (2,500–5,000 cells were counted per section, per mouse).

Results

Generation of *Pten*$^{L/L}$*;TPO-Cre* mice. To generate a model of *Pten* loss in the thyroid follicular cells, we crossed $Pten^{L/L}$ mice, harboring two *loxP* sites flanking *Pten* exons 4 and 5 (23), with transgenic mice expressing the Cre recombinase under the control of the human TPO promoter (Fig. 1*A*; ref. 22). TPO-Cre mice express the recombinase in most thyrocytes, starting between 14.5 and 16.6 d.p.c., when the mouse thyroid enters the final steps of differentiation expressing thyroglobulin, thyroid peroxidase, and sodium-iodide symporter (25).

PCR analysis of different tissues, using primers selectively amplifying the unrecombined or the recombined allele, showed that *Pten* was specifically deleted in the thyroids of mice expressing Cre (Fig. 1*B*; data not shown). To quantitate the deletion efficiency in the $Pten^{L/L}$*;TPO-Cre* thyroids, we compared the amount of the intact *Pten* allele with that of the recombined allele by quantitative PCR (24). In agreement with previous reports (24), no recombination was detected in other tissues (data not shown). Approximately 70% and 90% of the floxed alleles had undergone recombination in 10- and 45-week-old mice, respectively (Fig. 1*C*). We did not detect any recombined product in Cre-negative samples, whereas *Pten* deletion reached, as expected, 100% in T-cell lymphomas from

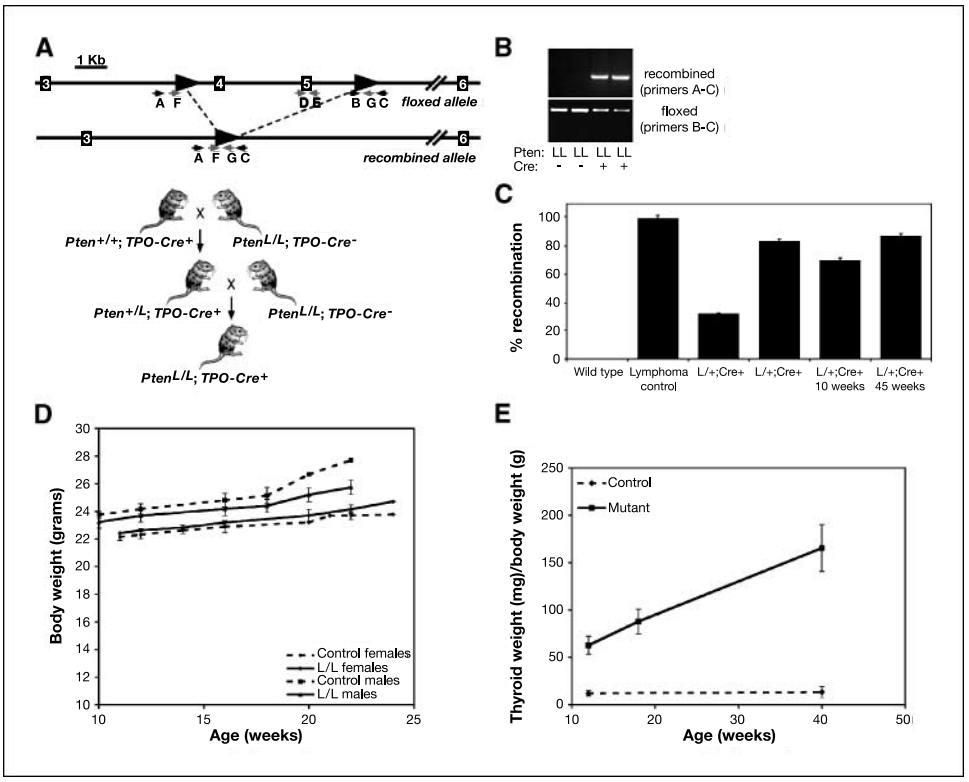

Figure 1. Characterization of *Pten*$^{L/L}$*;TPO-Cre* mice. *A,* representation of the floxed *Pten* locus before and after Cre-mediated recombination. *Arrows,* primers for genotyping. *B,* PCR approach showing the appearance of a recombination-specific product in the thyroids expressing Cre. *C,* estimation of *Pten* recombination efficiency. The ratio of the recombined allele is shown as a percentage of the total (unrecombined and recombined) alleles, set at 100%. *D,* weight gain of control and mutant mice over 12 wks, showing normal growth rate. *E,* age-dependent enlargement of the thyroids in the *Pten*$^{L/L}$*;TPO-Cre* mice. *Bars*, SD.

Pten$^{L/L}$ mice that express Cre in the thymus (Fig. 1*C*). Taking into account the presence of unrecombined alleles deriving from the thyroid endothelium and from C cells, we can assume that the thyrocyte recombination efficiency in this model approaches 100%.

Pten$^{L/L}$*;TPO-Cre* mice were born at the expected Mendelian ratios and developed normally, achieving sexual maturity without displaying obvious physical or behavioral abnormalities. No significant differences in body weight gain between wild-type (WT) and mutant mice were found in a 20-week follow-up (Fig. 1*D*; data not shown).

Goiter development in *Pten*$^{L/L}$*;TPO-Cre* mice. WT and *Pten*$^{L/L}$*;TPO-Cre* littermates were sacrificed at different time points, starting at 10 weeks of age, to assess the effect of *Pten* deletion on the thyroid gland. At all time points, the mutant thyroids, irrespective of gender, were strikingly enlarged compared with WT glands (Figs. 1*E* and 2*A* and *B*). At 10 weeks of age, the average weight of mutant thyroids, adjusted for the body weight, was already increased five times compared with controls (Fig. 1*E*). In addition, whereas the growth of WT thyroids slows down drastically after ~10 weeks from birth, *Pten*$^{L/L}$*;TPO-Cre* glands continued to increase in size and their normalized weight, at 40 weeks of age, was on average 12 times larger than controls (Fig. 1*E*).

The analysis of H&E-stained sections from 10- to 18-week-old mice showed that the increased gland size was associated with a widespread follicular enlargement and that the follicles were homogeneously filled with colloid (Fig. 2*C* and *D*). To verify that *Pten* expression had been completely abrogated, we did immunohistochemical detection of Pten and of the active form of Akt (pAkt), which is increased as a result of *Pten* deletion. WT glands showed strong Pten reactivity in both the cytoplasm and the nucleus of the follicular cells, which was completely abolished in the mutant glands. C cells and endothelial cells were still immunoreactive, thus providing additional evidence of the thyrocyte specificity of *Pten* ablation (Fig. 2*E* and *F*). pAkt was expressed at low levels in the nucleus and cytoplasm of control thyrocytes. However, loss of *Pten* resulted in a dramatic increase in the pAkt immunoreactivity of these cells (Fig. 2*G* and *H*). These findings are in sharp contrast with the normal thyroid size and structure that characterizes *Pten*$^{+/-}$ mice at the same age (data not shown). Thus, activation of Akt in the thyroid follicular cells, as a consequence of complete *Pten* ablation, results in the early development of diffuse colloid goiter.

To determine whether the goiter developing in *Pten*$^{L/L}$*;TPO-Cre* mice is associated with an altered hormonal milieu, we measured serum levels of TSH and T4 by radioimmunoassay in a group of 10- to 13-week-old WT and *Pten*$^{L/L}$*;TPO-Cre* mice (n = 10). As expected, TSH levels in the female mice were about half of those in the males; however, no significant differences in the levels of TSH and T4 were detected between control and mutant mice (Fig. 3*A* and *B*). These data show that *Pten*$^{L/L}$*;TPO-Cre* mice are euthyroid and suggest that the defects leading to goiter development do not result in an increase of thyroid hormone synthesis by the follicular cells, thus preserving the negative feedback loop regulating TSH production from the pituitary.

To analyze in detail the morphologic changes induced by loss of *Pten*, we determined the average number of follicles per square millimeter in a cohort of age-matched (10–12 weeks) WT and mutant mice. Irrespective of their sex, *Pten*$^{L/L}$*;TPO-Cre* mice displayed a striking decrease (>50%) in follicle density compared with controls (Fig. 3*C*). Reduced follicle density was primarily caused by generalized follicle enlargement, again irrespective of the mouse gender: mutant follicles were on average three times as large as their WT counterparts (Fig. 3*D*).

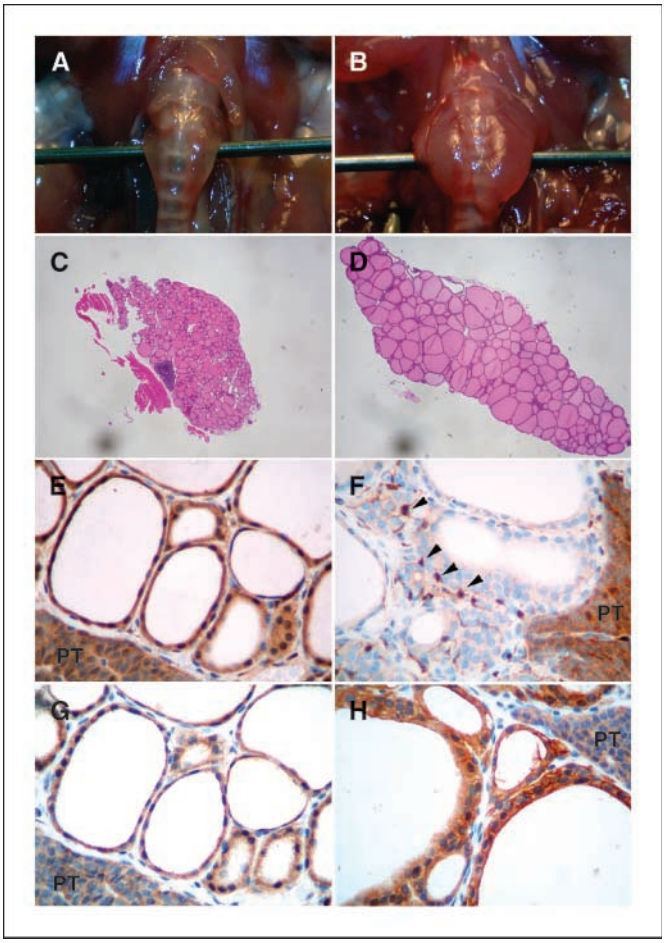

Figure 2. Thyromegaly in *Pten*$^{L/L}$*;TPO-Cre* mice. *A* to *D,* comparison of representative thyroids from control (*A* and *C*) and mutant (*B* and *D*) 10-wk-old mice. Magnification, ×40 (*C* and *D*). *E* to *H,* immunohistochemical detection of Pten (*E* and *F*) and activated Akt (*G* and *H*) in the thyroid of control (*E* and *G*) and mutant (*F* and *H*) 10-wk-old mice. Note the complete loss of Pten expression in the mutant thyroid, with the exception of the parathyroid (*PT*) and a few endothelial and C cells (*arrowheads*). Magnification, ×400 (*E–H*).

Increased proliferation in *Pten*$^{L/L}$*;TPO-Cre* thyrocytes. Microscopic examination of WT and mutant thyroids revealed a subtle but reproducible and statistically significant phenotypic difference between male and female mutant mice. In fact, the cell density of mutant males (follicular cells per square millimeter) was reduced ~30% compared with control males (Figs. 3*E* and *G* and 4*A*), reflecting the fact that, in the mutant mice, the follicular lumen is increased. Conversely, the female thyroids had the same cell density as their WT counterparts, despite the fact that male and female mutant thyroids have similarly enlarged follicles. Thus, this difference in cell density must reflect a net increase in total follicular cell number in the females (Figs. 3*F* and *H* and 4*A*).

To start understanding the mechanism behind this differential increase in cellularity between genders, we measured the proliferation of follicular cells in WT and *Pten*$^{L/L}$*;TPO-Cre* thyroids at 12 to 15 weeks of age using an antibody against the proliferation marker Ki-67. WT mice have, at this age, a very low proliferation index, irrespective of gender. However, the proliferation of mutant follicular cells was strikingly different between male and female

thyroids. Male *Pten*$^{L/L}$*;TPO-Cre* mice had on average a 3-fold increase in follicular proliferation, whereas female mutants displayed a 6-fold increase (Fig. 4*B* and *C*). Taken together, these data show that the enlarged follicles developing as a consequence of *Pten* loss are in part due to increased thyrocyte proliferation and that this effect is more marked in the females.

Signaling cascades activated by *Pten* loss. The development of thyroid hyperplasia with full penetrance in young *Pten*$^{L/L}$*;TPO-Cre* mice makes it possible to analyze *in vivo*, in a genetically defined model, the pathways that are altered as a result of *Pten* loss and that thus contribute to goiter pathogenesis and increased proliferation rate. We used immunohistochemistry to investigate the expression levels and phosphorylation status of several proteins acting in pathways directly affected by Akt activation and found that both p70S6K1 and its major target, ribosomal protein S6, were highly phosphorylated and thus activated in mutant follicular cells compared with controls (Fig. 4*D*). In addition, the transcription factor Foxo1, a direct target of Akt, was phosphorylated and delocalized to the cytoplasm in mutant thyroids (Fig. 4*D*). *Pten*$^{L/L}$*;TPO-Cre* thyroids also displayed increased nuclear levels of cyclin D1, thus establishing a causative link with the increased proliferation rates observed in the mutant thyroids (Fig. 4*D*). Western blot analysis revealed a strong increase in the expression levels of cyclin D3, whereas the expression of p27 remained substantially unaltered (Fig. 4*E*).

To gain insight into the mechanism(s) behind the gender differences in cellularity and proliferation detected in mutant mice, we stained control and mutant thyroids with antibodies recognizing ERα and its Ser^{167}-phosphorylated form, which is a direct target

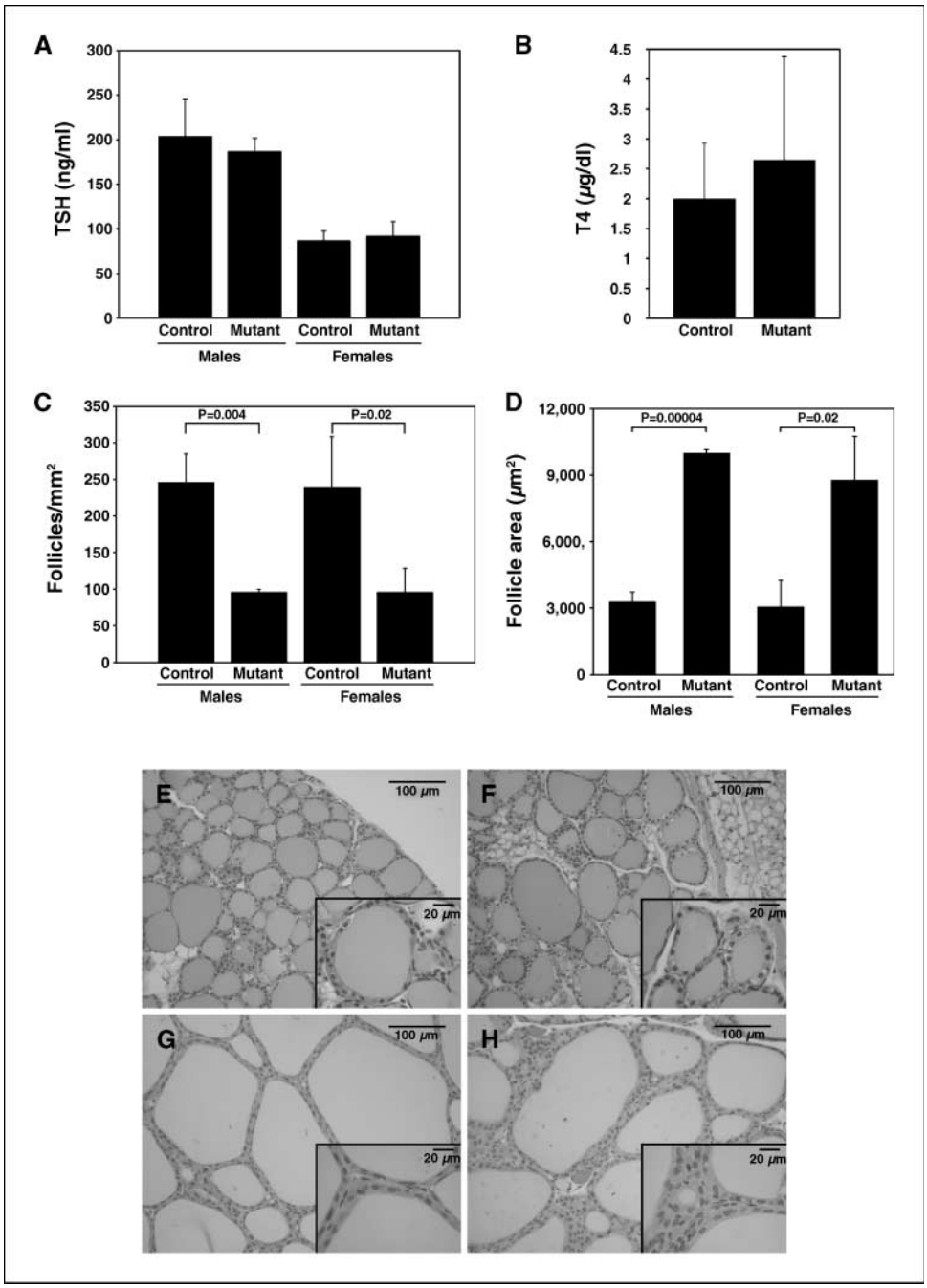

Figure 3. Hormonal and morphometric characterization of *Pten*$^{L/L}$*;TPO-Cre* mice. *A* and *B*, TSH and T4 levels in control and mutant mice (n = 5, 10–13 wks old). *C*, follicle density in control and mutant mice. *D*, mean follicle area in control and mutant mice. *E* to *H*, enlarged follicles in 10-wk old *Pten*$^{L/L}$*;TPO-Cre* mutant mice. Representative microphotographs from control male (*E*) and female (*F*) mice and from *Pten*$^{L/L}$*;TPO-Cre* male (*G*) and female (*H*) mice. Magnification, ×100. Magnification, ×400 (*insets*). *Bars*, SD.

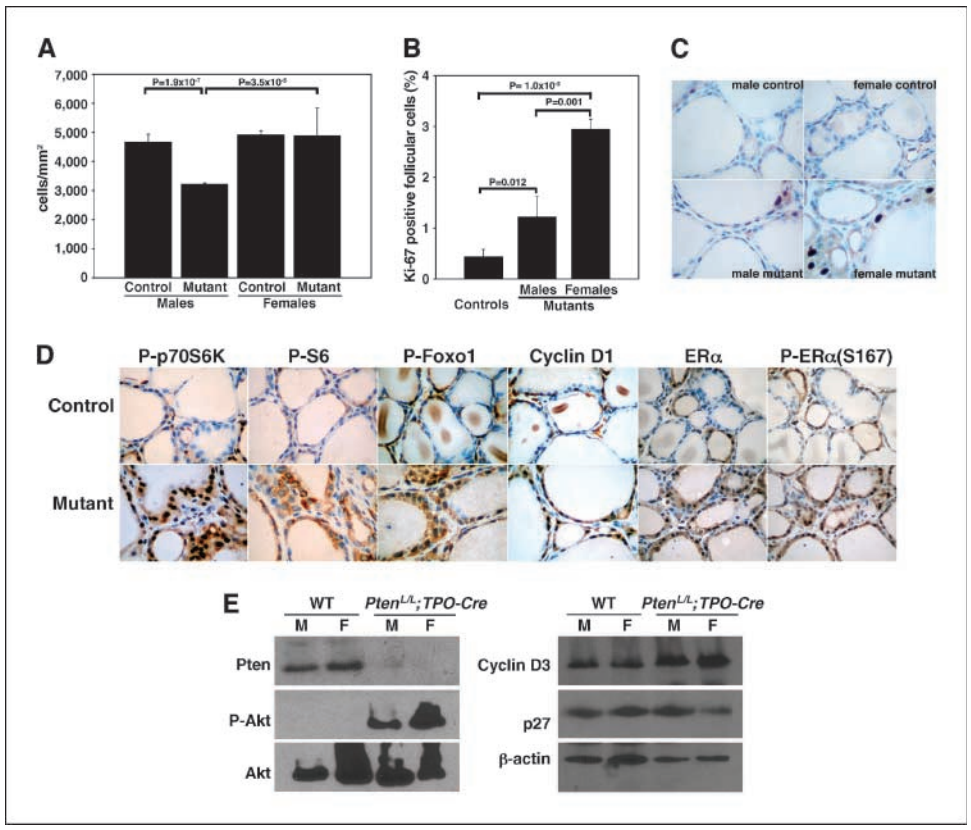

Figure 4. Increased thyrocyte proliferation in *Pten*$^{L/L}$*;TPO-Cre* mice. *A,* cell density in control and mutant mice showing increased cellularity in the thyroids of female mutants. *B* and *C,* proliferative index of control and mutant thyrocytes, determined by Ki-67 immunohistochemistry. *D* and *E,* immunohistochemical (*D*) and Western blot (*E*) analysis of the expression levels of several proteins involved in the increased proliferation observed in the mutant thyroids. Magnification, ×400. *Bars*, SD.

of Akt and has increased transcriptional activity compared with nonphosphorylated receptor, thus potentially contributing to the differences in proliferation between male and female mutants. Immunoreactivity for ERα and P-ERα was restricted to scattered follicles and patches of thyrocytes in WT mice. However, *Pten*$^{L/L}$*;TPO-Cre* thyroids showed a striking increase in the number of follicular cells positive for both ERα and P-ERα compared with controls (Fig. 4*D*), suggesting that *Pten* loss might result in the expansion of an ERα^{+} population or, less likely, in an increase of ERα expression. These data show that *Pten* loss in the mouse thyroid activates several pathways that can cooperatively contribute to the increased proliferation and overall organ growth characterizing *Pten*$^{L/L}$*;TPO-Cre* thyroids.

Elevation of TSH levels minimally increases the proliferation and growth of *Pten*$^{L/L}$*;TPO-Cre* thyroids. TSH constitutes the major growth signal for thyroid cells. Activation of TSHR primarily initiates the cAMP signaling cascade. However, several conflicting data exist on the involvement of other pathways, including the PI3K/Akt cascade, downstream of activated TSHR, and on the extent of the contribution to thyrocyte proliferation of these pathways. We reasoned that if the contribution of PI3K/Akt to proliferation was additive to the other pathways initiated by TSH, such as cAMP/PKA and Ras/MAPK, then supraphysiologic TSH levels should lead to a further increase in the proliferation of the *Pten* mutant cells.

To boost TSH-dependent thyroid stimulation, control and mutant mice were subjected to a 4-week treatment with the goitrogens methimazole and sodium perchlorate, which increase TSH secretion by decreasing thyroid hormone synthesis. As expected, the weight of treated thyroids was increased 3-fold in WT mice, irrespective of gender, compared with untreated controls. However, unexpectedly, goitrogen treatment did not further augment the weight of the *Pten*$^{L/L}$*;TPO-Cre* thyroids over the 5- to 6-fold increase deriving from *Pten* ablation (Fig. 5*A, B*, and *E*). WT goitrous thyroids showed a striking reduction of the follicle area with almost complete disappearance of the follicular structure (Fig. 5*C*). However, the thyroids of *Pten*$^{L/L}$*;TPO-Cre* mice still displayed rather large follicular lumina despite goitrogen treatment (Fig. 5*D*). In addition, remarkable thyrocyte hypertrophy characterized both genotypes.

In agreement with the thyroid weight data, the proliferation index of control goitrogen-stimulated glands was increased almost 7-fold compared with WT follicular cells, with no gender difference. Thyroids from treated male mutants had a 4-fold higher mitotic index compared with untreated male mutants and reached the same levels as treated females. However, the proliferation index of goitrogen-treated female *Pten*$^{L/L}$*;TPO-Cre* mice was only minimally increased compared with untreated mutant females (Fig. 5*F*). These data suggest that the PI3K/Akt cascade conveys a major proliferative signal in thyroid follicular cells, even under strong TSH stimulation, and that unrestrained PI3K activity is sufficient to obtain near-maximal proliferation in female mice.

***Pten*$^{L/L}$*;TPO-Cre* mice develop thyroid adenomas.** To determine whether loss of *Pten* is sufficient to induce the development of neoplastic lesions, a cohort of mice was aged to 8 to 10 months and then sacrificed. At this age, the mutant thyroids were still growing (Fig. 1*E*) and still characterized by diffuse goiter with enlarged colloid-filled follicles (Fig. 6*A–C*). Additionally, all mice now showed focal hyperplasia, small nonencapsulated areas of hypercellularity with solid and/or microfollicular patterns, variable nuclear atypia, and little or no colloid among the dilated follicles of the colloid goiter (Fig. 6*A–C*). In addition, 70% of the female mice

developed well-circumscribed follicular adenomas, often encapsulated, characterized by increased cellularity, severe reduction of the follicular areas resulting in a microfollicular and solid pattern, and the presence of mild nuclear atypia and several mitotic figures (Fig. 6*A–F*). The follicular nature of these lesions was confirmed by absence of calcitonin staining (data not shown).

The proliferation index of the nonneoplastic thyroid areas was, as in younger mice, significantly increased compared with control mice, again with a more severe increase in the females (Fig. 6*G* and *H*). Strikingly, the hyperplastic and adenomatous areas showed a further 5-fold proliferation increase, irrespective of sex, and with a wide variability between individual lesions, even within the same gland (Fig. 6*H*). In comparison, the thyroids from age-matched *Pten*$^{+/-}$ mice displayed only scattered hyperplastic or small nodular lesions, characterized by complete loss of Pten expression, in an otherwise normal background (Fig. 6*I*; Table 1; data not shown). These results suggest that *Pten* loss creates a fertile environment for the development of highly proliferative neoplastic lesions, as a result of focal, clonal genetic alterations that act in cooperation with the activation of Akt.

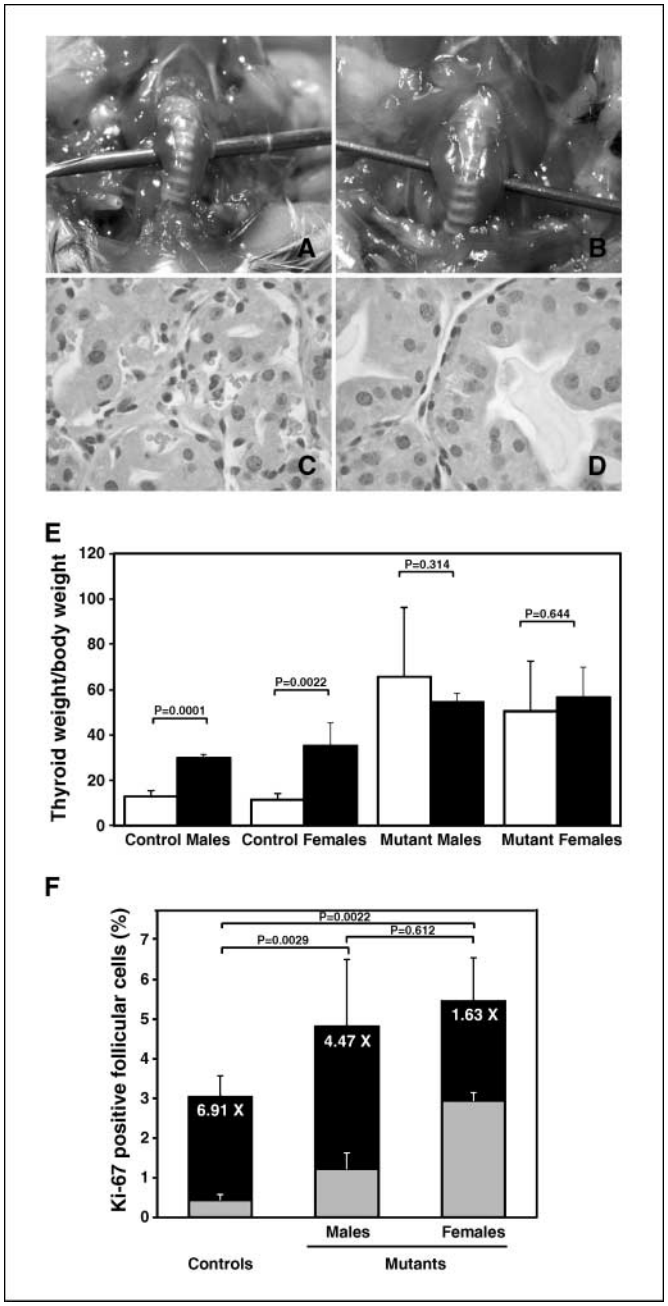

Figure 5. Goitrogen treatment does not increase the hyperplasia of *Pten*$^{L/L}$*;TPO-Cre* thyroids. Comparison of a representative thyroid from control (*A* and *C*) and mutant (*B* and *D*) 12-wk-old mice, after 4 wks of treatment. Magnification, ×400 (*C* and *D*). *E,* goitrogen-dependent enlargement of the thyroids. *White columns,* untreated mice; *black columns,* goitrogen-treated mice. *F,* proliferative index of control and goitrogen-treated thyrocytes, determined by Ki-67 immunohistochemistry. *Gray* and *black columns,* untreated and goitrogen-treated mice, respectively. *Bars*, SD.

Discussion

The identification of the central signaling nodes in the cascades involved in thyrocyte growth and division is vital to understand the pathogenetic mechanisms of thyroid proliferative disorders, from simple goiter to thyroid carcinoma. *In vitro* and *in vivo* approaches have helped establish that TSH is the major driving force for thyroid growth and function (7). However, the relative contribution of the different TSH-initiated cascades to the various aspects of thyroid physiology and growth is still largely unknown. In fact, the different cell models used to dissect these pathways have often led to contradictory results (7).

One major unresolved issue is the extent of the contribution of PI3K/Akt pathway to thyrocyte proliferation, as a direct or indirect downstream effector of TSH. This question is particularly relevant in view of some striking divergences between clinicopathologic data and several *in vitro* studies.

Numerous clinical data point to the PI3K/Akt pathway as a major player in thyroid neoplastic transformation. Inherited *PTEN* mutations lead to Cowden disease, characterized by thyroid multinodular goiter and adenoma, and increased risk for thyroid cancer (18–20); in addition, activation of Akt (14) and gain-of-function mutations of *PIK3CA*, encoding the catalytic subunit of PI3K (13), have been correlated to thyroid carcinoma progression. PTEN subcellular distribution seems to shift from nuclear to cytoplasmic during neoplastic progression, before the dramatic reduction that characterizes advanced thyroid tumors (26) and, in follicular tumors, the localization of activated Akt is inversely correlated to the presence of PTEN in the nucleus (27).

However, whereas rat thyroid cells in culture seem to require PI3K activation downstream TSH stimulation for proliferation (7), TSH effectors, cAMP and PKA, cannot activate PI3K or Akt in dog primary thyrocytes, a system in which the PI3K/Akt pathway does not seem to be involved in TSH-mediated thyrocyte proliferation (11).

In this study, we have used a genetic model of *Pten* loss and constitutive Akt activation in thyroid follicular cells to investigate the role of the PI3K/Akt cascade in thyrocyte proliferation and in neoplastic transformation. The *Pten*$^{L/L}$*;TPO-Cre* mice can be considered both as a model of Cowden disease, in which loss of heterozygosity at the WT locus results in goiter and adenomas (28), and as a tool to investigate the connection between PI3K activation and sporadic goiter pathogenesis. Although more in-depth studies are necessary to define the *Pten*$^{L/L}$*;TPO-Cre* mice as a faithful model of human disease, they represent the first genetically defined model designed to examine the role of increased PI3K signaling in thyroid disease without resorting to nonphysiologic overexpression. Studies conducted using transgenic mice overexpressing members of the IGF-I pathway (29, 30) have resulted in mild

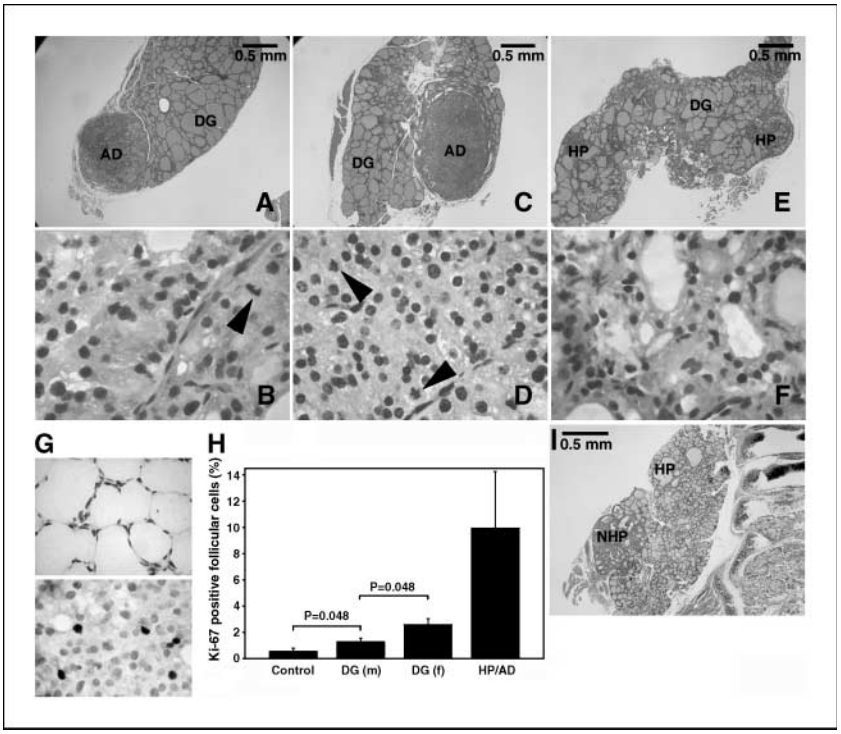

Figure 6. Hyperplastic lesions and adenomas in *Pten*$^{L/L}$*;TPO-Cre* mice. *A* to *C,* thyroid sections (magnification, ×40) from 10 mo old *Pten*$^{L/L}$*;TPO-Cre* mice showing adenomas (*AD*) and hyperplasia (*HP*) in the context of diffuse goiter (*DG*). *D* to *F,* magnification (×400) of the lesions shown in (*A–C*), showing microfollicular growth and mitotic figures (*arrowheads*). *G* and *H,* proliferative index of control and mutant thyrocytes, determined by Ki-67 IHC. *I*, nodular (*NHP*) and hyperplastic (*HP*) lesions arising in *Pten*$^{+/-}$ mice. *Bars*, SD.

phenotypes, and overexpression of members of the TSHR/cAMP pathway have reinforced the notion that TSH delivers, *in vivo,* the main proliferative signal for thyroid follicular cells (31–33).

Our data strongly suggest that activation of PI3K, in the absence of any alteration of TSH levels, is sufficient to induce a high rate of thyrocyte proliferation and the development of goiter. Several PI3K/Akt effectors were found activated in mutant thyroids. The p70S6K1/S6 axis has been suggested to play an essential role in thyroid proliferation and activity downstream TSH (34). Indeed, *Pten*$^{L/L}$*;TPO-Cre* thyroids were characterized by highly phosphorylated p70S6K1 and S6 proteins, suggesting that PI3K activation is sufficient to stimulate this pathway. We also found that PI3K/Akt activation was associated with increased levels of both cyclin D1 and cyclin D3, consistent with previous data supporting their role in thyrocyte proliferation and human thyroid proliferative disorders (35, 36).

Interestingly, activation of the PI3K signaling cascade was not associated to a reduction of p27Kip1 levels. Although this is in contrast with previous data linking Akt activation to p27Kip1 expression (37), it is tempting to speculate that safeguard mechanisms are in place to retain p27Kip1 levels to constrain the proliferative signals triggered by Akt activation. Later, on the other hand, loss of p27Kip1 expression might shift this compromised equilibrium toward proliferation, leading to malignant transformation as shown in human thyroid disease (38) and in a *Pten*$^{+/-}$*;p27Kip1*$^{-/-}$ mouse model (39).

Strikingly, the increased proliferation characterizing *Pten*$^{L/L}$*;TPO-Cre* thyrocytes is more pronounced in females than males, mimicking the increased prevalence of thyroid disorders among women (40). Although more in-depth studies will be necessary to elucidate the exact mechanism responsible for the greater proliferative response in the mutant females, and its relevance to human disease, our data suggest that the activation of the PI3K/Akt/ERα axis, in the presence of physiologic levels of estrogen, may contribute to this phenotype, extending our recent findings obtained in an endometrial cancer model (41). It is also noteworthy that mutant thyroids show phosphorylation and delocalization of Foxo1, which has been reported to act as an ERα repressor (42).

It has been proposed that TSH can induce local IGF-I production and thus activate IGF-I receptor (IGF-IR) and its downstream cascades (43). In fact, several data in the literature point to a role of IGF-I in thyroid growth, either in parallel to or downstream TSH (7). In addition, thyroid enlargement is present in the majority of patients with acromegaly (44), and transgenic mice coexpressing

Table 1. Prevalence and histologic characteristics of follicular alterations in *Pten*$^{+/-}$ and *Pten*$^{L/L}$*;TPO-Cre* mice

Genotype	Sex	No.	Age (wk)	Normal (%)	Focal hyperplasia (%)	Nodular hyperplasia (%)	Adenoma (%)
Pten$^{+/-}$	Male	15	28–64	13.3	46.7	40	0
	Female	14	26–56	14.3	35.7	50	0
Pten$^{L/L}$*;TPO-Cre*	Male	8	33–44	0	0	100*	0
	Female	7	34–45	0	0	28.6*	71.4*

*In a context of diffuse goiter.

IGF-I and IGF-IR develop diffuse goiter (29). Our data show that constitutive activation of one major IGF-IR effector, PI3K, induces a phenotype that is qualitatively similar, although quantitatively much more dramatic, to IGF-I/IGF-IR mice, underlining the relevance of this pathway to thyroid disease. Furthermore, we found that pathologically increased levels of TSH could only slightly increment the mitotic index of mutant thyrocytes, with no increase in the mutant gland weight, strongly suggesting that a conspicuous part of the proliferation signal induced by TSH is funneled through the PI3K/Akt cascade.

Despite the proliferative disorder in the thyroids of young *Pten*$^{L/L}$*;TPO-Cre* mice and the development of adenomas in several older mice, none of the mutants had developed invasive lesions by 11 months of age, showing that activation of the PI3K/Akt pathway is not sufficient for thyroid malignant transformation. Current studies are aimed at defining the identity of the genetic lesions that can cooperate with *Pten* loss to promote invasive tumor formation.

In summary, our data show that the PI3K/Akt cascade conveys a major proliferative signal in thyroid follicular cells that is sufficient to obtain near-maximal proliferation, at least in the females, and to induce the development of goiter and nodular thyroid lesions.

Acknowledgments

Received 9/22/2006; revised 11/10/2006; accepted 11/21/2006.

Grant support: Commonwealth of Pennsylvania to the Fox Chase Cancer Center (FCCC) and a National Cancer Institute core grant (FCCC).

The costs of publication of this article were defrayed in part by the payment of page charges. This article must therefore be hereby marked *advertisement* in accordance with 18 U.S.C. Section 1734 solely to indicate this fact.

We thank Dr. Maureen Murphy for critical reading of the manuscript and FCCC for the Transgenic, DNA Synthesis, Laboratory Animal, and Biomarker facilities.

References

1. Saad AG, Kumar S, Ron E, et al. Proliferative activity of human thyroid cells in various age groups and its correlation with the risk of thyroid cancer after radiation exposure. J Clin Endocrinol Metab 2006;91:2672–7.
2. Ezzat S, Sarti DA, Cain DR, Braunstein GD. Thyroid incidentalomas. Prevalence by palpation and ultrasonography. Arch Intern Med 1994;154:1838–40.
3. Rivas M, Santisteban P. TSH-activated signaling pathways in thyroid tumorigenesis. Mol Cell Endocrinol 2003;213:31–45.
4. Larsen PR. Thyroid-pituitary interaction: feedback regulation of thyrotropin secretion by thyroid hormones. N Engl J Med 1982;306:23–32.
5. Dremier S, Coulonval K, Perpete S, et al. The role of cyclic AMP and its effect on protein kinase A in the mitogenic action of thyrotropin on the thyroid cell. Ann N Y Acad Sci 2002;968:106–21.
6. Bidey SP, Hill DJ, Eggo MC. Growth factors and goitrogenesis. J Endocrinol 1999;160:321–32.
7. Kimura T, Van Keymeulen A, Golstein J, Fusco A, Dumont JE, Roger PP. Regulation of thyroid cell proliferation by TSH and other factors: a critical evaluation of *in vitro* models. Endocr Rev 2001;22:631–56.
8. Bellacosa A, Kumar C, Di Cristofano A, Testa JR. Activation of AKT kinases in cancer: implications for therapeutic targeting. Adv Cancer Res 2005;94:29–86.
9. Di Cristofano A, Pandolfi PP. The multiple roles of PTEN in tumor suppression. Cell 2000;100:387–90.
10. Saito J, Kohn AD, Roth RA, et al. Regulation of FRTL-5 thyroid cell growth by phosphatidylinositol (OH) 3 kinase-dependent Akt-mediated signaling. Thyroid 2001;11:339–51.
11. Coulonval K, Vandeput F, Stein RC, Kozma SC, Lamy F, Dumont JE. Phosphatidylinositol 3-kinase, protein kinase B and ribosomal S6 kinases in the stimulation of thyroid epithelial cell proliferation by cAMP and growth factors in the presence of insulin. Biochem J 2000;348 Pt 2:351–8.
12. Motti ML, Califano D, Troncone G, et al. Complex regulation of the cyclin-dependent kinase inhibitor p27kip1 in thyroid cancer cells by the PI3K/AKT pathway: regulation of p27kip1 expression and localization. Am J Pathol 2005;166:737–49.
13. Garcia-Rostan G, Costa AM, Pereira-Castro I, et al. Mutation of the PIK3CA gene in anaplastic thyroid cancer. Cancer Res 2005;65:10199–207.
14. Ringel MD, Hayre N, Saito J, et al. Overexpression and overactivation of Akt in thyroid carcinoma. Cancer Res 2001;61:6105–11.
15. Eng C. Role of PTEN, a lipid phosphatase upstream effector of protein kinase B, in epithelial thyroid carcinogenesis. Ann N Y Acad Sci 2002;968:213–21.
16. Tell G, Pines A, Arturi F, et al. Control of phosphatase and tensin homolog (PTEN) gene expression in normal and neoplastic thyroid cells. Endocrinology 2004;145:4660–6.
17. Alvarez-Nunez F, Bussaglia E, Mauricio D, et al. PTEN promoter methylation in sporadic thyroid carcinomas. Thyroid 2006;16:17–23.
18. Nelen MR, van Staveren WC, Peeters EA, et al. Germline mutations in the PTEN/MMAC1 gene in patients with Cowden disease. Hum Mol Genet 1997;6:1383–7.
19. Bussaglia E, Pujol RM, Gil MJ, et al. PTEN mutations in eight Spanish families and one Brazilian family with Cowden syndrome. J Invest Dermatol 2002;118:639–44.
20. Sogol PB, Sugawara M, Gordon HE, Shellow WV, Hernandez F, Hershman JM. Cowden's disease: familial goiter and skin hamartomas. A report of three cases. West J Med 1983;139:324–8.
21. Di Cristofano A, Pesce B, Cordon-Cardo C, Pandolfi PP. Pten is essential for embryonic development and tumour suppression. Nat Genet 1998;19:348–55.
22. Kusakabe T, Kawaguchi A, Kawaguchi R, Feigenbaum L, Kimura S. Thyrocyte-specific expression of Cre recombinase in transgenic mice. Genesis 2004;39:212–6.
23. Trotman LC, Niki M, Dotan ZA, et al. Pten dose dictates cancer progression in the prostate. PLoS Biol 2003;1:385–96.
24. Kusakabe T, Kawaguchi A, Hoshi N, Kawaguchi R, Hoshi S, Kimura S. Thyroid-specific enhancer-binding protein/NKX2.1 is required for the maintenance of ordered architecture and function of the differentiated thyroid. Mol Endocrinol 2006;20:1796–809.
25. De Felice M, Postiglione MP, Di Lauro R. Thyrotropin receptor signaling in development and differentiation of the thyroid gland: insights from mouse models and human diseases. Endocrinology 2004;145:4062–7.
26. Gimm O, Perren A, Weng LP, et al. Differential nuclear and cytoplasmic expression of PTEN in normal thyroid tissue, and benign and malignant epithelial thyroid tumors. Am J Pathol 2000;156:1693–700.
27. Vasko V, Saji M, Hardy E, et al. Akt activation and localisation correlate with tumour invasion and oncogene expression in thyroid cancer. J Med Genet 2004;41:161–70.
28. Marsh DJ, Dahia PL, Coulon V, et al. Allelic imbalance, including deletion of PTEN/MMACI, at the Cowden disease locus on 10q22-23, in hamartomas from patients with Cowden syndrome and germline PTEN mutation. Genes Chromosomes Cancer 1998;21:61–9.
29. Clement S, Refetoff S, Robaye B, Dumont JE, Schurmans S. Low TSH requirement and goiter in transgenic mice overexpressing IGF-I and IGF-IR receptor in the thyroid gland. Endocrinology 2001;142:5131–9.
30. Modric T, Rajkumar K, Murphy LJ. Thyroid gland function and growth in IGF binding protein-1 transgenic mice. Eur J Endocrinol 1999;141:149–59.
31. Coppee F, Gerard AC, Denef JF, et al. Early occurrence of metastatic differentiated thyroid carcinomas in transgenic mice expressing the A2a adenosine receptor gene and the human papillomavirus type 16 E7 oncogene. Oncogene 1996;13:1471–82.
32. Ribeiro-Neto F, Leon A, Urbani-Brocard J, Lou L, Nyska A, Altschuler DL. cAMP-dependent oncogenic action of Rap1b in the thyroid gland. J Biol Chem 2004;279:46868–75.
33. Zeiger MA, Saji M, Gusev Y, et al. Thyroid-specific expression of cholera toxin A1 subunit causes thyroid hyperplasia and hyperthyroidism in transgenic mice. Endocrinology 1997;138:3133–40.
34. Suh JM, Song JH, Kim DW, et al. Regulation of the phosphatidylinositol 3-kinase, Akt/protein kinase B, FRAP/mammalian target of rapamycin, and ribosomal S6 kinase 1 signaling pathways by thyroid-stimulating hormone (TSH) and stimulating type TSH receptor antibodies in the thyroid gland. J Biol Chem 2003;278:21960–71.
35. Saiz AD, Olvera M, Rezk S, Florentine BA, McCourty A, Brynes RK. Immunohistochemical expression of cyclin D1, E2F-1, and Ki-67 in benign and malignant thyroid lesions. J Pathol 2002;198:157–62.
36. Motti ML, Boccia A, Belletti B, et al. Critical role of cyclin D3 in TSH-dependent growth of thyrocytes and in hyperproliferative diseases of the thyroid gland. Oncogene 2003;22:7576–86.
37. Medema RH, Kops GJ, Bos JL, Burgering BM. AFX-like forkhead transcription factors mediate cell-cycle regulation by Ras and PKB through p27kip1. Nature 2000;404:782–7.
38. Erickson LA, Yousef OM, Jin L, Lohse CM, Pankratz VS, Lloyd RV. p27kip1 expression distinguishes papillary hyperplasia in Graves' disease from papillary thyroid carcinoma. Mod Pathol 2000;13:1014–9.
39. Di Cristofano A, De Acetis M, Koff A, Cordon-Cardo C, Pandolfi PP. Pten and p27KIP1 cooperate in prostate cancer tumor suppression in the mouse. Nat Genet 2001;27:222–4.
40. Libutti SK. Understanding the role of gender in the incidence of thyroid cancer. Cancer J 2005;11:104–5.
41. Vilgelm A, Lian Z, Wang H, et al. Akt-mediated phosphorylation and activation of estrogen receptor α is required for endometrial neoplastic transformation in Pten$^{+/-}$ mice. Cancer Res 2006;66:3375–80.
42. Zhao HH, Herrera RE, Coronado-Heinsohn E, et al. Forkhead homologue in rhabdomyosarcoma functions as a bifunctional nuclear receptor-interacting protein with both coactivator and corepressor functions. J Biol Chem 2001;276:27907–12.
43. Tode B, Serio M, Rotella CM, et al. Insulin-like growth factor-I: autocrine secretion by human thyroid follicular cells in primary culture. J Clin Endocrinol Metab 1989;69:639–47.
44. Gasperi M, Martino E, Manetti L, et al. Prevalence of thyroid diseases in patients with acromegaly: results of an Italian multi-center study. J Endocrinol Invest 2002;25:240–5.

Pten Loss in the Mouse Thyroid Causes Goiter and Follicular Adenomas: Insights into Thyroid Function and Cowden Disease Pathogenesis

Nicole Yeager, Andres Klein-Szanto, Shioko Kimura, et al.

Cancer Res 2007;67:959-966.